

## METHOD

# Reconstructing large interaction networks from empirical time series data

Chun-Wei Chang<sup>1,2</sup>  | Takeshi Miki<sup>3,4,5</sup>  | Masayuki Ushio<sup>6,7</sup>  | Po-Ju Ke<sup>8,9</sup>  |  
Hsiao-Pei Lu<sup>10</sup>  | Fuh-Kwo Shiah<sup>2,3</sup> | Chih-hao Hsieh<sup>1,2,3,9</sup> 

<sup>1</sup>National Center for Theoretical Sciences, Taipei, Taiwan

<sup>2</sup>Research Center for Environmental Changes, Academia Sinica, Taipei, Taiwan

<sup>3</sup>Institute of Oceanography, National Taiwan University, Taipei, Taiwan

<sup>4</sup>Faculty of Advanced Science and Technology, Ryukoku University, Otsu, Japan

<sup>5</sup>Center for Biodiversity Science, Ryukoku University, Otsu, Japan

<sup>6</sup>Hakubi Center, Kyoto University, Kyoto, Japan

<sup>7</sup>Center for Ecological Research, Kyoto University, Otsu, Japan

<sup>8</sup>Department of Ecology and Evolutionary Biology, Princeton University, Princeton, New Jersey, USA

<sup>9</sup>Institute of Ecology and Evolutionary Biology, National Taiwan University, Taipei, Taiwan

<sup>10</sup>Department of Biotechnology and Bioindustry Sciences, National Cheng Kung University, Tainan, Taiwan

**Correspondence**

Chih-hao Hsieh, Institute of Oceanography, National Taiwan University, Taipei, Taiwan.  
Email: chsieh@ntu.edu.tw

**Funding information**

National Taiwan University; National Center for Theoretical Sciences; Foundation for the Advancement of Outstanding Scholarship; Ministry of Science and Technology

**Editor:** Serguei Saavedra

**Abstract**

Reconstructing interactions from observational data is a critical need for investigating natural biological networks, wherein network dimensionality is usually high. However, these pose a challenge to existing methods that can quantify only small interaction networks. Here, we proposed a novel approach to reconstruct high-dimensional interaction Jacobian networks using empirical time series without specific model assumptions. This method, named “multiview distance regularised S-map,” generalised the state space reconstruction to accommodate high dimensionality and overcome difficulties in quantifying massive interactions with limited data. When evaluating this method using time series generated from theoretical models involving hundreds of interacting species, estimated strengths of interaction Jacobians were in good agreement with theoretical expectations. Applying this method to a natural bacterial community helped identify important species from the interaction network and revealed mechanisms governing the dynamical stability of a bacterial community. The proposed method overcame the challenge of high dimensionality in large natural dynamical systems.

**KEYWORDS**

dynamical stability, interaction network, microbial community, network topology

**INTRODUCTION**

An interaction network critically determines the dynamics and stability of dynamical systems (Albert et al., 2000; Strogatz, 2001). Therefore, statistical tools for analysing network properties have been well-developed (Barrat et al., 2004). However, quantitative recovery of interaction networks from natural systems remains

challenging, in particular, to identify and quantify network edges (i.e., interactions between network nodes). For instance, identifying trophic interactions in food webs relies on direct observations, for example, gut content analysis (Morinière et al., 2003) or indirect molecular approaches, for example, stable isotope analysis (Fry, 2006). These approaches are labour-intensive and have limited resolution to identify and quantify interactions

in large networks. Other types of interactions, such as competition and facilitation, are difficult to quantify in real-world systems and can only be investigated within a small number of interacting species (Griffin et al., 2004). Consequently, it becomes extremely difficult to reconstruct high-dimensional interaction networks consisting of enormous numbers of nodes (e.g., microbes living in natural ecosystems and proteins in cells) and edges (e.g., competition/facilitation between microbial species and activation/inactivation of proteins).

More recently, empirical dynamic modelling (EDM) based on state space reconstruction (SSR) of dynamical attractor was proposed to quantify interactions in nonlinear dynamical systems. EDM, such as multivariate S-map; (Deyle et al., 2016), have been developed to quantify time-varying interaction Jacobians requiring no model assumptions. However, S-map allows only a limited number of variables (or network nodes) being embedded into the model (Deyle et al., 2016; Ushio et al., 2018). Consequently, S-map can only reveal interactions among a small number of species that is often much less than the network dimensionality (i.e., the number of interacting nodes, denoted as  $m$  hereafter). This restriction arises due to the “curse of dimensionality” (Bellman, 1957). Specifically, the data required to reconstruct tangent space of SSR grows exponentially

with system dimensionality, and thus makes data too sparse to correctly depict neighbouring relationships among data points (Hastie et al., 2009), whereas a correct neighbourhood relationship is essential for applying SSR-based methods (Ye & Sugihara, 2016). A modified S-map approach (Cenci et al., 2019) incorporating regularisation, while addressing the issue of process noise and potentially useful in estimating high-dimensional parameters (Hastie et al., 2009), is nevertheless still subject to the curse of dimensionality (Yu et al., 2020). Although several other methods were proposed to infer high-dimensional microbial networks (Bucci et al., 2016; Fisher & Mehta, 2014; Stein et al., 2013), these methods require assumptions on model structure (e.g., generalised Lotka-Volterra model), which is difficult to be verified for natural systems. Consequently, a nonparametric (or equation-free) method to reconstruct high-dimensional interaction networks for natural systems is still lacking.

Here, we propose a novel equation-free approach to reconstruct high-dimensional, time-varying interaction networks in large, nonlinear dynamical systems (e.g., ecological communities). The advantage of our approach is developing a novel distance measure (Figure 1) that quantifies the neighbouring relationships among high-dimensional data points in SSR. We refer to this measure as “multiview distance” because it is determined

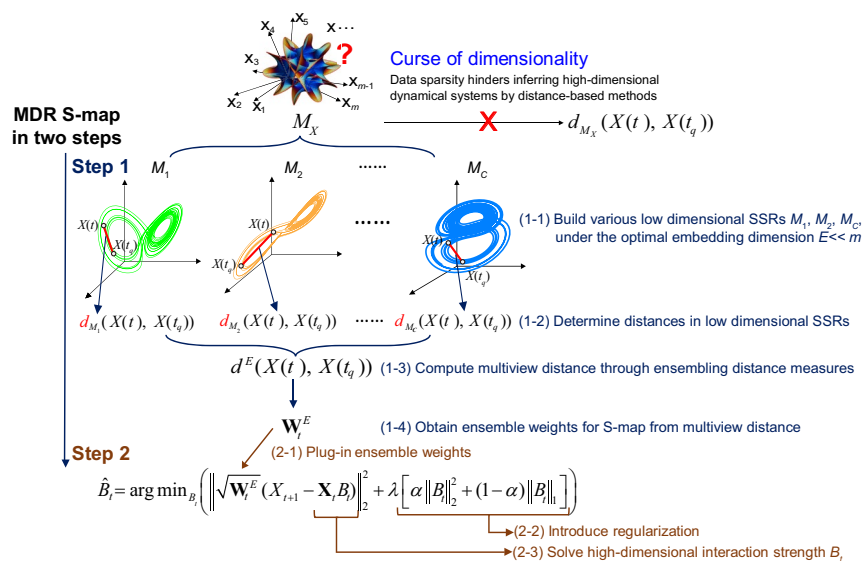


**FIGURE 1** Schematic illustration for MDR S-map analysis procedure. The MDR S-map consists of two steps. The aim of the first step is to obtain the multiview distance that operates at the optimal embedding dimension ( $E$ ) that is much smaller than the dimensionality of large interaction networks ( $m =$  number of nodes). Under the curse of dimensionality, neighbourhood relationships among data points cannot be precisely inferred from the distance,  $d_M(\cdot)$  among high-dimensional data points in manifold  $M_X$  that summarises the dynamics of entire interaction networks. Therefore, (1–1) we recovered the neighbourhood relationships among high-dimensional data points  $X(t)$  from numerous low-dimensional state space reconstruction (SSR;  $M_1, M_2, \dots, M_C$ ) (i.e., multiview SSR). Among these SSRs, (1–2) we computed distances ( $L^2$  norm, i.e., Euclidean distance) between data points under the optimal embedding dimension  $E$ . Collecting all these distances, (1–3) we obtained the multiview distances ( $d^E$ ) and (1–4) determined the data weights ( $W^E$ ) for the following S-map analysis. In the second step, we estimated the high-dimensional interaction strength ( $B$ ) by S-map, based on locally weighted least square optimisation ( $\arg \min_B (\|\cdot\|_2^2)$ ) with regularisation ( $\lambda[\cdot]$ ) incorporated. Specifically, (2–1) the weights,  $w_i^E = \exp(-\theta d^E / \text{mean}(d^E))$ , derived in the first step were plugged-in the S-map optimisation algorithm. (2–2) Under the constraint of regularisation ( $\lambda$  and  $\alpha$  are the penalty factors of regularisation). (2–3) we solved the high-dimensional local linear coefficients to approximate interaction strengths at each time step. Detailed definitions of each variable are reported in Methods and SI Text, I. *MDR S-map algorithm and implementation*

by ensembling numerous distances measured in various low-dimensional, topologically equivalent SSRs (i.e., multiview embeddings; [Ye & Sugihara, 2016]). Through multiview distance, our approach links two existing EDM methods, multiview embedding (Ye & Sugihara, 2016) and regularised S-map (Cenci et al., 2019), to reconstruct large interaction networks, but avoids problems associated with high dimensionality by conducting SSR operations under the optimal embedding dimension ( $E$ ) much smaller than network dimensionality  $m$  (i.e.,  $E \ll m$ ). This method, named “multiview distance regularised S-map” (abbreviated as MDR S-map, hereafter), is summarised in two steps (Figure 1): (i) measuring multiview distances among  $m$ -dimensional data from various  $E$ -dimensional multiview SSR that embeds various combinations of variables (Ye & Sugihara, 2016); and (ii) determining  $m$ -dimensional interaction Jacobian matrix at each time point by plugging-in multiview distances to S-map algorithm with regularisation constraints (Cenci et al., 2019) (Methods and SI Text, *I. MDR S-map algorithm and implementation*). More detailed statistical properties of MDR S-map are in SI Text, *II. Statistical properties of MDR S-map*. Through the two-step procedure of MDR S-map, we aim to reconstruct high-dimensional interaction networks for large dynamical systems using time series data.

It is noteworthy that the interaction strength quantified by MDR S-map as well as other EDM approaches is the interaction Jacobian (Berlow et al., 2004), not the interaction coefficient. Interaction coefficient is the parameter describing per capita effect of one species  $j$  to the other species  $i$  (e.g., the parameter  $\alpha_{ij} = \partial(\frac{1}{x^{(i)}} \frac{dx^{(i)}}{dt}) / \partial x^{(j)}$  in generalised Lotka-Volterra model, where  $x^{(i)}$  is the abundance of species  $i$  and  $t$  is time) and is more often used in previous network studies than interaction Jacobian, especially in theoretical analysis (Allesina & Levine, 2011; Dunne et al., 2002). However, interaction Jacobian (e.g.,  $J_{ij} = \frac{\partial x^{(i)}(t+1)}{\partial x^{(j)}(t)}$  in discrete-time systems) recovered by our algorithm quantifies the net effects of abundance changes in nodes  $j$  (between two consecutive observations) on the abundance of species  $i$ , which is more consistent with the findings of empirical addition/removal experiments (Carpenter & Kitchell, 1988; Skelly, 2002). The interaction Jacobian is time-varying as it integrates two sources of temporal variability: (i) species abundance changed with time; and (ii) the interaction coefficient is time-varying (i.e.,  $\alpha_{ij} = \alpha_{ij}(t)$ ; e.g., McCoy and Pfister [2014]). Nevertheless, reconstructing interaction Jacobians remains meaningful in determining the dynamic behaviour of the system (Cenci & Saavedra, 2019; Ushio et al., 2018) and provides a powerful tool to empirically track temporal variations in interaction (Deyle et al., 2016), which might be critical to the urgent issue concerning how ecological networks would respond to environmental changes (Hoegh-Guldberg & Bruno, 2010).

We tested the MDR S-map method using simulated time-series data mainly from a stochastic population dynamic model (i.e., multi-species Ricker model in Methods and SI Text, *III. Parameterisation of multi-species Ricker model with random noises*), where interaction strengths and network properties are exactly known. Then, we employed this method to analyse empirical bacterial community data (dominant OTUs [operational taxonomic units]) collected from a natural coastal environment (Martin-Platero et al., 2018). In both simulated and empirical datasets, numbers of selected species (i.e.,  $m = 117$  and 136 for synthetic data from multi-species Ricker model and empirical bacterial community data, respectively) were more than the length of time series data ( $N = 100$  and 90 for synthetic and empirical data, respectively), a situation that very likely occurs in real-world datasets concerning large interaction networks. Based on analysis of a bacterial community, we demonstrated a real-world application of MDR S-map for reconstructing large, time-varying interaction networks and unveiling the interplay among network properties, dynamics, and stability.

## MATERIALS AND METHODS

### *MDR S-map*

Our method of reconstructing large interaction networks using time series data was based on EDM, an approach rooted in attractor reconstruction (Chang et al., 2017). Regarding the latter, a critical parameter is the optimal embedding dimension,  $E$ , that determines how many time-lags or variables were incorporated in SSR-based methods (Deyle et al., 2016; Hsieh et al., 2005; Kennel et al., 1992; Shalizi, 2006; Ye & Sugihara, 2016). In large systems, classical methods encounter an issue: the number of network nodes is much greater than what EDM models can accommodate [ $E$  usually  $< 20$  (Hsieh et al., 2005)]. To overcome this difficulty, we proposed a method, MDR S-map, that allows estimating interaction strengths of high-dimensional systems while maintaining the SSR operation at the low-dimensional,  $E$ . Figure 1 summarised the two-step analytical procedure based on state space reconstruction and more detailed algorithms, implementation, and statistical properties of MDR S-map were provided in SI Text, *I. MDR S-map algorithm and implementation* and *II. Statistical properties of MDR S-map*. In addition to inferring interaction Jacobians, the proposed new method, similar with other EDM methods (Cenci et al., 2019; Deyle et al., 2013; Sugihara et al., 1990; Sugihara & May, 1990), enables to forecast the future states of model variables in chaotic systems. Therefore, we also compared MDR S-map with existing EDM methods regarding their forecast ability.

### ***Assessing MDR S-map based on a theoretical network model***

We validated our MDR S-map approach mainly by analysing time series data generated from a theoretical network model, multi-species Ricker model, where the interaction strengths and network quantitative features are known *a priori*. This network model initially consists of 1000 interacting species. Let  $N_i(k)$  denote the population size of species  $i$  ( $i = 1, 2, \dots, 1000$ ) at time step  $t$  ( $t = 0, 1, 2, \dots, n$ ), and  $\mathbf{N}(t) = (N_1(t), N_2(t), \dots, N_{1000}(t))^T$ . Population dynamics of species  $i$  followed the discrete-time equation,

$$N_i(t+1) = N_i(t) \exp [r_{0i} (1 + e_i \mathbf{M}\mathbf{N}(t))] \quad (1)$$

where  $r_{0i}$  is the intrinsic growth rate of species  $i$ ,  $e_i$  is a vector taking zero values for all except for the  $i$ th entity,  $\mathbf{M}$  represents time-independent interaction matrix with the size  $1000 \times 1000$  (with elements  $m_{ij}$  representing the effect of species  $j$  on species  $i$ ). The detail parameterisation of the multi-species Ricker model was offered in SI Text, III.

### ***Parameterisation of multi-species Ricker model with random noises***

For model time series, we only used the last 100 time steps of the 1000 simulated steps for further analyses. Because only some of the model populations in this chaotic system could sustain their dynamics until the end of model computations, we only selected dominant species with mean relative abundance  $>0.1\%$  (calculated over the last 100 steps) for further analyses. These dominant species had obvious temporal fluctuations, which is necessary for applying EDM. Then, we applied the MDR S-map to reconstruct the interaction networks from the simulated time series and compared the reconstructed networks to theoretical networks derived from the Jacobian matrix of the difference equation model. To make reasonable comparisons, we multiplied the theoretical expectation of Jacobian  $\left(\frac{\partial X_{t+1}}{\partial Y_t}\right)$  by the ratio of standard deviations,  $\frac{\sigma_Y}{\sigma_X}$ , because time series data were normalised with respect to the temporal standard deviations prior to performing MDR S-map. Finally, we examined whether the estimated interaction Jacobians were consistent with the scaled theoretical Jacobians.

Based on the reconstructed interaction networks, we verified whether interaction strengths (interaction Jacobians) can be successfully recovered at each time point. Specifically, we computed inference skill that was defined as the Pearson correlation between all theoretical and estimated interaction strengths. We determined the inference skill at each time point and investigated how inference skill varied among time-varying

interaction Jacobian matrices. In addition, we calculated node inference skills defined as the averaged inference skill on evaluating the interactions associated with each single species, including the interactions that a species imposes on others (outward) or be affected by others (inward).

In addition, we examined the quantitative features of interaction Jacobian networks reconstructed from data generated by the multi-species Ricker model. To verify the quantitative features of entire interaction networks, we calculated mean and standard deviation of interaction strength. We also evaluated key measures derived from interaction Jacobian matrices, including its trace and dominant eigenvalue, which characterises dynamical behaviour of dynamical systems (Cenci & Saavedra, 2019; Ushio et al., 2018). In summary, we derived quantitative measures describing interaction networks from various aspects to test whether topological properties in theoretical networks were quantitatively preserved in the reconstructed networks.

### ***Sensitivity tests of MDR S-map on more complicated data structure and alternative network models***

We tested the robustness of MDR S-map on random noises and data issues that are common in real world applications: (1) only percentage data are available; (2) impacts of data noise (including process and observation noise and stochastic environmental forcing); and (3) not all data from every network node are available (incomplete network nodes). These were incorporated in the synthetic data generated by the multi-species Ricker model. Then, we examined the influences of these complexities on inferring interaction Jacobians.

In addition, to test whether MDR S-map can reconstruct interaction networks without specific model assumption (i.e., nonparametric), we examined the inference skills of MDR S-map on reconstructing interaction Jacobians of more complicated network models. In addition to the (i) multi-species Ricker model, we also tested MDR S-map on (ii) discrete Lotka-Volterra competition model, (iii) Ricker-Beverton-Holt model, and (iv) host-parasitoid Nicholson-Bailey model. Moreover, we additionally incorporated time-varying interaction coefficients with seasonal variations into all these models. In total, we examined the inference skills on inferring interaction Jacobians in eight network models (i.e., four model types (i–iv) with either fixed or time-varying interaction coefficients). Time series datasets produced from these models were based on the same procedure as that for the multi-species Ricker model. The details of these models were presented in SI Text, IV. *Testing MDR S-map on more complicated network models.*



## Analysis of empirical bacterial time series data

We applied MDR S-map on an empirical time series dataset of natural bacterial communities in Canoe Beach, Boston, MA, USA (Martin-Platero et al., 2018). This dataset was derived from 16S rRNA gene amplicon-sequencing data sampled daily from July 23, 2010 to October 23, 2010. In total, there were 90 valid time points, apart from three interrupted missing data. In this dataset, only relative abundances were available for bacteria OTUs. To be consistent with analysis of model time series, we selected the dominant species (mean relative abundance > 0.1%). In total, 136 OTUs were selected. Due to data limitations, we reconstructed bacterial interaction networks using relative abundance data; nevertheless, based on our analysis using the model example, the network reconstruction using percentage data was still reliable to a large extent (See our discussion in SI Text, II-2. *Statistical properties of MDR S-map based on percentage data*).

The reconstructed interaction networks enabled us to explore how and why the bacterial interaction network changed over time. Here, we investigated causal mechanisms underlying dynamical stability of the bacterial community. Specifically, we examined causal relationships between the trace of reconstructed Jacobian matrices that was referred as an practical index indicating structural instability (Cenci & Saavedra, 2019) versus summary network statistics (e.g., mean interaction strength), ecological properties characterising bacterial diversity (e.g., Shannon diversity) and physicochemical environments (e.g., nutrients and salinity). To examine their relationships, we applied linear analysis (temporal correlation) to determine the statistical association and nonlinear analysis (CCM) to identify causality. For linear correlation analysis, we calculated the Pearson correlation coefficient between pairs of time series and tested the significance using a stationary bootstrap that accommodates autocorrelations in time series. For nonlinear causality test, we performed CCM analysis (Chang et al., 2017) (See the section *Identifying causal variables by CCM* in SI Text, I-1).

## Computation

All analyses were done with R (ver. 3.1.2). Simplex projection and CCM analyses were implemented using the rEDM (Version 1.2.3) package (Ye et al., 2013). The elastic-net regularisation used in MDR S-map is solved by glmnet package (version 3.0). Network topological properties were computed using the igraph package (Csardi & Nepusz, 2006). The computation codes of MDR S-map, as well as other analytical procedures, are deposited in the Figshare Repository (<https://doi.org/10.6084/m9.figshare.16573037.v1>; [Chang et al., 2021]).

## RESULTS AND DISCUSSION

### *One-step forward predictability of network nodes and optimal regularisation algorithms*

Prior to analysing the reconstructed networks, we evaluated the forecasting ability of MDR S-map for the dynamics of network nodes (e.g., one-step forward forecast of future node states), as forecasting skills represent a proxy of reliability for reconstructed dynamical systems (Ye & Sugihara, 2016) and are highly associated with inference skills on inferring interactions (Figure S1). Compared to other EDM methods, MDR S-map had greater forecasting skills than other EDM methods (Table 1). In addition, for model time series generated by the multi-species Ricker model, the MDR S-map outperformed all other EDM methods (Table 1), irrespective of regularisation algorithms (i.e., classical [Hastie et al., 2009] and adaptive [Zou & Zhang, 2009] elastic-net regularisation). Similarly, the MDR S-map outperformed other EDM methods in empirical bacteria time series (Table 1). Specifically, the MDR S-map results, based on classical elastic-net regularisation, had the best performance in both in-sample and out-of-sample forecasts. The MDR S-map results, based on adaptive elastic-net regularisation, also outperformed all existing EDM methods for out-of-sample forecasts, but had similar performance as the regularised S-map for in-sample forecasts (Table 1). It is noteworthy that existing EDM methods (e.g., multivariate and regularised S-map) performed reasonably well and have been demonstrated to outperform other linear time series analyses on forecasting nonlinear dynamical systems (Deyle et al., 2013; Sugihara et al., 1990). Nevertheless, our proposed MDR S-map further improved forecast skills, as full information of entire networks was incorporated, whereas only partial information of sub-networks can be incorporated by other EDM approaches. Although this improvement was not tremendous, the novel findings based on incorporating complete networks likely open a new research direction for future development of nonlinear time series analysis. Nevertheless, forecast skills of MDR S-map decreased with spanning forecast horizon (at the most 20 steps forward presented in Figure S2) because forecast errors would be accumulated and amplified, especially in chaotic systems as revealed in other EDM methods (Sugihara et al., 1990).

Although MDR S-map can effectively forecast dynamics of network nodes, irrespective of regularisation algorithms, adaptive elastic-net regularisation obtained less false-positive findings in estimating interaction strengths for simulated data and thus was applied to reconstruct interaction networks throughout our analyses in this study. Compared to the MDR S-map analysis based on adaptive elastic-net, the analysis based on classical elastic-net had slightly better forecast skills, but less accuracy and more false-positive findings in its

TABLE 1 Comparison of forecast performance among various EDM methods

Data	Forecast skill	Type of evaluation	Univariate S-map	Multivariate S-map	Regularised S-map (classical elastic-net)	MDR S-map (classical elastic-net)	MDR S-map (adaptive elastic-net)
Model	Pearson $r$	In-sample	0.75 ± 0.14	0.81 ± 0.12	0.83 ± 0.11	<b>0.996 ± 0.01</b>	0.99 ± 0.01
		Out-of-sample	—	—	—	—	—
	rMSE	In-sample	0.61 ± 0.17	0.54 ± 0.19	0.52 ± 0.18	<b>0.08 ± 0.05</b>	0.13 ± 0.05
		Out-of-sample	0.71 ± 0.37	0.67 ± 0.38	0.66 ± 0.39	<b>0.09 ± 0.08</b>	0.14 ± 0.09
	MAE	In-sample	0.47 ± 0.14	0.42 ± 0.14	0.39 ± 0.13	<b>0.06 ± 0.03</b>	0.09 ± 0.04
		Out-of-sample	0.63 ± 0.35	0.60 ± 0.33	0.59 ± 0.34	<b>0.08 ± 0.07</b>	0.13 ± 0.08
Bacterial community	Pearson $r$	In-sample	0.48 ± 0.21	0.58 ± 0.18	0.62 ± 0.19	<b>0.70 ± 0.13</b>	0.63 ± 0.18
		Out-of-sample	—	—	—	—	—
	rMSE	In-sample	0.90 ± 0.43	0.80 ± 0.16	0.75 ± 0.15	<b>0.70 ± 0.15</b>	0.78 ± 0.20
		Out-of-sample	0.48 ± 0.58	0.49 ± 0.43	0.51 ± 0.45	<b>0.41 ± 0.42</b>	0.41 ± 0.43
	MAE	In-sample	0.54 ± 0.16	0.50 ± 0.13	0.47 ± 0.12	<b>0.44 ± 0.11</b>	0.48 ± 0.13
		Out-of-sample	0.44 ± 0.55	0.45 ± 0.41	0.47 ± 0.42	<b>0.38 ± 0.40</b>	0.38 ± 0.41

Note: Three types of forecast skill, Pearson  $r$  correlation coefficient, rMSE (root mean square error), and MAE (mean absolute error), were calculated and averaged for all individual nodes. Here, we summarised the computed forecast skills as mean ± SD. Irrespective of forecast skill types, the MDR S-map had the best performance in both leave-one-out cross-validation (in-sample) and out-of-sample forecasts. The Pearson  $r$  for out-of-sample forecast was not calculated, as only two test samples were used in this analysis. Bold values label the optimal results based on various forecast skills. The model evaluation was made for the Ricker model.

interaction strength estimations (accuracy = 0.671 and 0.863 and false positive rate = 0.308 and 0.029, based on classical and adaptive elastic-net regularisations, respectively; Table S1). The adaptive elastic-net includes an additional penalty to eliminate small non-zero estimates that are potentially false positive (Zou & Zhang, 2009), whereas classical elastic-net does not eliminate nodes that have no direct interaction with the target node, but are still informative to forecast its future state (possibly through indirect interactions) (Ye et al., 2015). Based on this result, the best regularisation algorithm optimising one-step forecast was slightly different from that optimising network reconstructions. As our objective was to estimate interaction strengths, we only present results of network reconstruction based on adaptive elastic-net regularisation in the rest of this work.

### Evaluating the quality of reconstructed interaction network using simulated datasets

MDR S-map correctly quantified the strengths of time-varying interactions (i.e., Jacobians  $J_{ij}(t)$  quantifying the net influence of node  $j$  on  $i$  at time  $t$ ) in high-dimensional ( $m = 117$ ) interaction networks embedded in the multi-species Ricker model. The estimated interaction strengths were highly consistent with theoretical expectations derived from the model (Figure 2). Such strong consistency held in most analysed time points (Figure 2b,c) and in most network nodes (Figure 2d), as well as for out-of-sample data (Figure S3) and for the long-term median (Pearson  $r = 0.930$ ; Figure S4a) obtained from temporal medians of all interaction strengths (i.e., long-term  $J_{ij} = \text{median}(J_{ij}(t)); t = 1, 2, \dots, n$ ). In contrast, the theoretical long-term medians had a weak negative relationship with interaction strengths inferred from the correlation coefficients between each pair of time series (Pearson  $r = -0.081$  and  $p < 0.01$  in Figure S4b), suggesting that correlation between time series provided no clear information for knowing true interaction strength in nonlinear systems, as reported (Sugihara et al., 2012). Thus, although inferring interaction using correlation-based approaches remains common in ecology literature (Carr et al., 2019; Freilich et al., 2018), applying these methods requires careful check on their underlying assumptions (Berry & Widder, 2014; Carr et al., 2019). However, the strengths of weak interactions cannot be precisely estimated by MDR S-map, resulting in a substantial portion of false positive and false negative findings (Table S1) presented as the vertical and horizontal parts, respectively, of the crosses near the origin (Figure 2a).

### Quantitative features of interaction Jacobian network

The reconstructed interaction networks well preserved the quantitative features characterising entire interaction

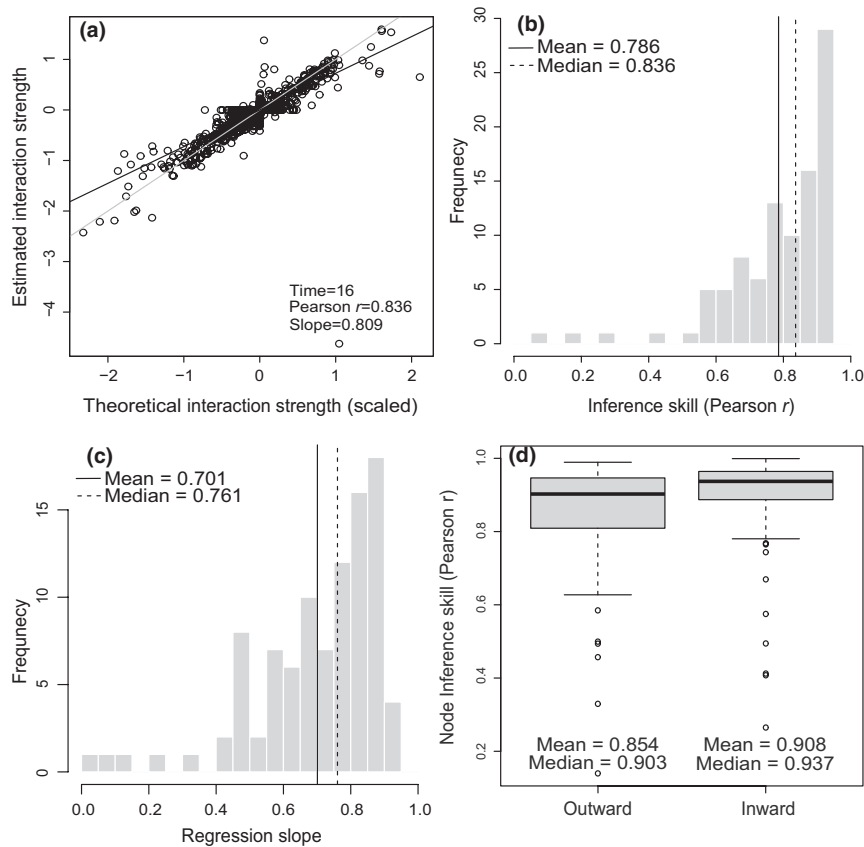


**FIGURE 2** Comparisons of interaction strengths estimated by MDR S-map, with true strengths derived from multi-species Ricker model. Interaction strengths (Jacobians) of time-varying interaction networks were effectively reconstructed with high inference skills (i.e., Pearson  $r$  examined at each time point). Panel (a) demonstrated an empirical linear relationship between the estimated and theoretical interaction Jacobians observed in a snapshot network at time =16, wherein the overall inference skill equals to the median value (0.836) among all inference skills. Here, grey line represents the 1:1 line, and black line represents the slope of simple linear regression. Applying this analysis presented in (a) for all time points, the distributions of inference skill (b) and regression slope (c) were determined. These distributions revealed that the interaction networks can be reliably reconstructed at most time points, but the interaction strengths were slightly underestimated (i.e., slope <1 in [c]) because of the regularisation applied in MDR S-map. Based on node inference skills computed for each 117 nodes (d), the reconstructed interactions associated with individual nodes (a node can affect others [outward] or be affected [inward]) were mostly reliable

Jacobian networks embedded in the multi-species Ricker model. Firstly, the mean and standard deviation of interaction strengths, although slightly underestimated, had temporal dynamics highly associated with the dynamics of theoretically expected values (Figure S5a,b). That is, quantitative features in reconstructed networks were relatively correct; in a practical sense, due to this high consistency, we inferred that our approach was capable of monitoring structural changes of interaction Jacobian networks in time. Similarly, quantitative features of interaction Jacobian matrix, such as matrix trace  $\text{Tr}(\mathbf{J})$ , had a strong positive linear association with the temporal dynamics of theoretical  $\text{Tr}(\mathbf{J})$  (Figure S5c). However, local Lyapunov instability (i.e., the norm of dominant eigenvalue; Figure S5d) only preserved a ranked but not a quantitative relationship, which exhibited a concordance in the phases of peaks and valleys but not in quantitative magnitude. These results were consistent with the previous findings that the eigenvalue was more difficult to be recovered than the trace (Cenci & Saavedra, 2019) and that evaluation of dynamical stability remains

challenging (Kéfi et al., 2019) for large dynamical systems. In addition to features characterising entire networks, other topological properties associated with network nodes, for example, strength (i.e., weighted degree) and centrality (Figure S5e–h and Table S2; SI Text, *V. Topological properties of interaction Jacobian networks*) were also preserved. Although these topological properties were conventionally evaluated in a network quantified by interaction coefficients instead of interaction Jacobians, deriving these measures in interaction Jacobian networks remains useful to identify important species with critical roles in interaction networks.

It is noteworthy that other EDM approaches were unable to recover entire networks, as these methods cannot accommodate a large number of interactions in SSR models. A recent study (Ushio, 2020) quantified interaction by increasing embedding dimension in regularised S-map (Cenci et al., 2019) with the number of causal nodes (i.e., not operating at the optimal embedding dimension). This method, although quantified individual interactions with moderate accuracy, generally

cannot accurately estimate quantitative features of large networks (Figures S6–S8; SI Text, *VI. Importance of embedding dimension in the estimation of network topology*).

### ***Sensitivity tests of MDR S-map on complicated data structure***

The inference skill of MDR S-map remained high when faced with complicated data structures similar to real world applications. First, estimations based on relative abundance (or percentage) data, a common format for biological datasets (e.g., metabarcoding data (Martin-Platero et al., 2018)), remained effective for inferring the interaction networks with subtle biases (Figure S9). Second, our estimates were also robust to random noises, including observation noises, process noises and stochastic environmental forcing (Figures S10–S13; SI Text, *III-3. Robustness of MDR S-map to noises*). Nonetheless, among various noise types, observation noises had relatively stronger impacts than other types of noises on inference skills. Finally, the consistency between MDR S-map estimations and theoretical expectations persisted, even when some critical network nodes (e.g., dominant species ranked in top 10% of abundance) were artificially removed from the analysis (Figure S14). Therefore, we inferred that the reconstruction of network subgraphs was still reliable, even if some critical nodes (Figure S14) or external environmental forcing (Figures S10–S11) were unobservable or excluded from analyses for practical reasons.

### ***Tests of MDR S-map on more complicated network models***

Apart from (i) multi-species Ricker model (Figure 2), MDR S-map reconstructed interaction Jacobians of more complicated network models, including (ii) discrete Lotka-Volterra competition model (Figure S15a–c), (iii) Ricker-Beverton-Holt model (Figure S15d–f), and (iv) host–parasitoid Nicholson-Bailey model (Figure S15g–i) with reasonable inference skills (medians of overall inference = 0.918, 0.470, and 0.568, for model (ii–iv), respectively). In addition, the interaction Jacobians were also reconstructed in models incorporating time-varying interaction coefficients (Figure S16) with no or small reductions in inference skill (medians of overall inference = 0.667, 0.896, 0.478 and 0.587, for model (i–iv), respectively). Overall, inference skills were highest for model (ii), which had similar complexity as the original Ricker model (Figure 2), but were lower for the other more complicated models (iii and iv). Nevertheless, the application of MDR S-map in these cases remained effective under no specific model assumption. That is, MDR S-map was a useful nonparametric (equation-free) method, suitable for analysing empirical datasets generated by unknown governing equations.

### ***Applications to a real-world example of bacteria community***

#### **Identifying important bacterial species from interaction networks**

As an empirical example, we reconstructed bacterial interaction networks (Movie S1) in a natural coastal environment. On average, important OTUs exerting strong positive effects on others (out-strength) mainly belonged to order Flavobacteriales and order Rhodobacterales (Figure S17), many members of which are copiotrophic species (Fuhrman et al., 2015) that grow rapidly in suitable environments and respond instantaneously to environmental changes. This result confirmed previous findings that Flavobacteriales are capable of degrading various polymers into more labile forms (González et al., 2008), which might benefit other co-existing bacterial species. Similarly, the results based on hub centrality index also revealed the importance of Flavobacteriales and Rhodobacterales as well as the other OTUs (e.g., Sphingobacteriales and Actinomycetales in Table S3) that occupied the central position of interaction networks. Although functions of these important OTUs have not been fully elucidated, our approach provided a promising way to identify the most critical players from a perspective of interaction network. It is noteworthy that the amplicon sequencing method (Martin-Platero et al., 2018) used to collect this bacteria dataset may have missed some important OTUs, due to incomplete DNA extraction and PCR biases. Nonetheless, the reconstructed sub-network without including every OTU may be still reliable, according to our assessment on simulated datasets (Figure S14).

#### **Deciphering causal mechanisms governing dynamical stability of communities**

Reconstruction of high-dimensional interaction networks revealed causal mechanisms underlying dynamical stability of natural bacterial communities. Firstly, we computed the trace of interaction Jacobian matrices  $\text{Tr}(J)$ , which has been considered a nonparametric index inferring structural instability for empirical systems (Cenci & Saavedra, 2019). This index was causally affected by mean interaction strength ( $p$ -value of CCM defined in Method,  $p_{\text{CCM}} = 0.027$  in Figure 3a) and exhibited a marginally significant negative association in their temporal dynamics (Pearson  $r = -0.250$ ,  $p_{\text{bootstrap}} = 0.098$ ). Because mean interaction strengths were mostly positive, this negative association implied that bacterial communities became more stable if more facilitative interactions occurred in communities. Moreover, facilitative interactions dominated the interaction networks under productive environments, as revealed by high concentrations of chlorophyll *a* (Figure 3b) and nutrients (e.g.,



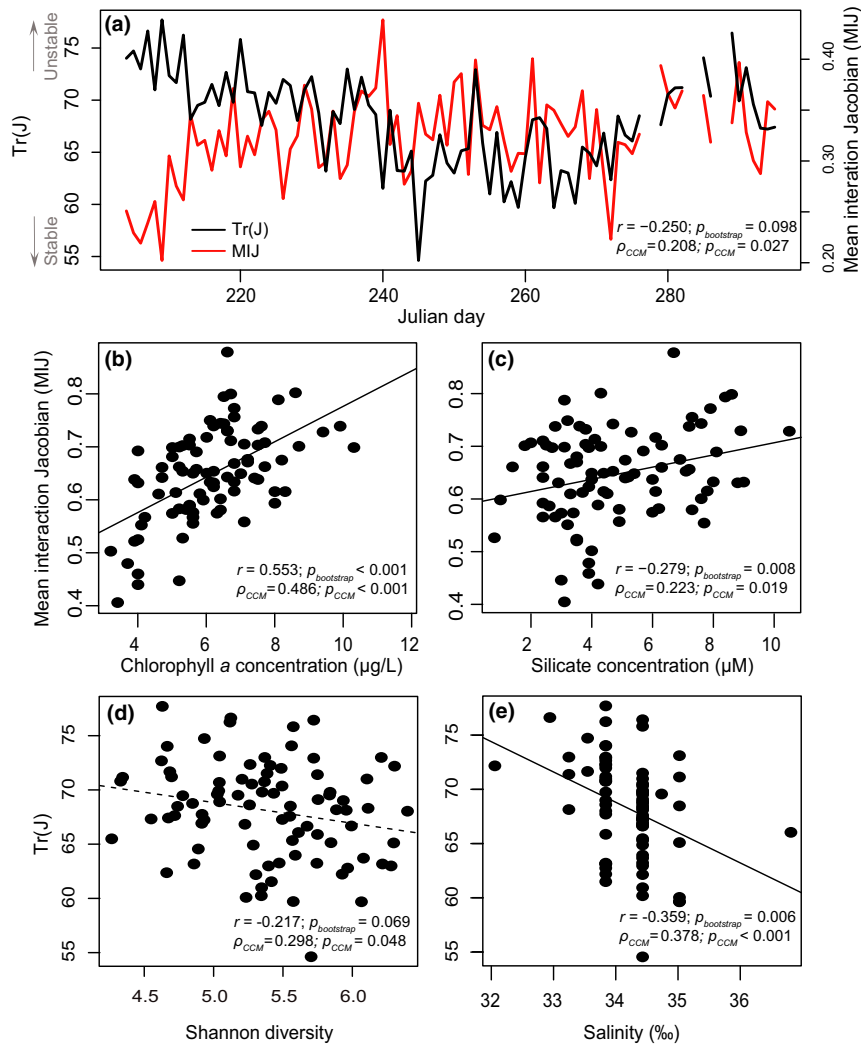


**FIGURE 3** Reconstructed interaction networks from empirical daily time series revealed causal mechanisms determining structural stability in a coastal bacterial community. (a) There was a significant negative association between mean interaction strength and the trace of reconstructed interaction Jacobian matrix,  $\text{Tr}(J)$ , that was used as a nonparametric measure for indicating structural instability (Cenci & Saavedra, 2019). In this system, there were more positive (facilitative) interactions when (b) primary production (approximated by chlorophyll a concentration) and (c) nutrient concentration (e.g., silicate) were high. Moreover,  $\text{Tr}(J)$  decreased with increasing Shannon diversity index (d). In addition, local environmental disturbances caused by terrestrial freshwater input destabilised the dynamics of marine bacterial community (e). Correlation analysis with stationary bootstrap ( $r$  and  $p_{\text{bootstrap}}$ ) and causality analysis with Convergent Cross Mapping ( $\rho_{\text{CCM}}$  and  $\rho_{\text{CCM}}$ ) were used to decipher mechanisms (see Methods)

silicate in Figure 3c). Likely, nutrients facilitated growth of primary producers producing abundant organic matters, which bring common benefits for various bacteria involved in various stages of organic decomposition and enhance facilitative interactions. In addition, the bacterial community was more structurally stable when the Shannon diversity of bacterial community was higher (Figure 3d), confirming previous findings of positive biodiversity effects on ecosystem stability (Chang et al., 2020). Apart from biological factors, structural stability was weakened by physicochemical disturbances caused by terrestrial freshwater input (revealed by reduced salinity in Figure 3e), a common local-scale disturbance in a coastal environment (Craft, 2007). These findings demonstrated a clear example elucidating key processes in

natural systems through uncovering network topology and stability measures, which could not be previously achieved due to lack of a method to reliably reconstruct large dynamical networks.

### Limitations in MDR S-map

There are several limitations in applying the MDR S-map algorithm. Firstly, the number of interactions cannot be exactly recovered, due to a lack of statistical power on inferring very weak interactions. Specifically, the number of interactions (i.e., edge number) detected in our reconstructed network was less than that in the model network (e.g., median edge number = 2098 and 889 for

theoretical and reconstructed networks in multi-species Ricker model, respectively). Consequently, the reconstructed network suffers from high false negative rate in identifying the presence of a weak interaction (Table S1). Nonetheless, errors for indicating wrong interaction sign rarely occurred. Therefore, our reconstructed network is unsuitable to uncover the topological properties relevant to link number (i.e., unweighted network), but is reliable to uncover quantitative properties weighted by interaction strength (i.e., weighted network) (Figure S5 and Table S2) that critically determine key properties of complex systems (Barbier et al., 2018; Liautaud et al., 2019). Nonetheless, future research is required to further improve the statistical power for correctly revealing weak interactions.

Although MDR S-map is an effective nonparametric method requiring no specific model assumption, inference skills are lower when analysing datasets generated by more complicated processes, for example, model incorporating time-varying interaction coefficients (Figure S16a–c), complex functional forms (e.g., Berveton-Holt model in Figure S15d–f), or more mechanistically formulated interactions (e.g., host-parasitoid model Figure S15g–i) compared to simple phenomenological models, such as a Ricker model (Figure 2). In addition, the application of our algorithm has been thus far limited to a few types of network models only, and robustness analyses were mainly conducted on the multi-species Ricker model. Therefore, it remains an open question about how efficiently the proposed method can reconstruct interaction networks with various complicated processes acting in concert (e.g., noises, complex interaction forms, types, or even higher order interactions [Levine et al., 2017]). Consequently, the proposed method, although it provides a novel methodological framework to address the curse of dimensionality, it still needs great effort to improve its efficiency via more detailed future investigations.

The algorithm might be less effective in reconstructing the networks with large ranges of interaction strength (Figure S18). This difficulty is caused by regularisation, which prevents large estimates in interaction strength due to including penalty on the magnitude of estimates. Thus, if some interaction strengths were too large, apparent inference errors appeared (Figure S18c) and destroyed the overall linear relationships between estimated and theoretical values. However, extremely strong interactions rarely exist in natural systems (McCann et al., 1998) and thus might not be very influential for empirical applications.

EDM-based methods, including MDR S-map, can so far be applied to investigate only interaction Jacobian networks. The reconstructed interaction Jacobians, although importantly determine system dynamics, are different from conventional networks quantified by fixed interaction coefficients. Theoretically, the interaction coefficients can be extracted from Jacobians by scaling abundances (with a specific assumption regarding

the governing equation, e.g., Ricker or generalised Lotka-Volterra model), but we do not recommend this procedure, as scaling of abundance is numerically unstable unless abundance can be precisely determined. Therefore, there is an urgent need to bridge the two types of interaction measures in theory, for example, theoretical analysis conducted by Song and Saavedra (2021), or to develop novel network theory established on interaction Jacobian networks that are empirically more available.

Considering the limitations in applying MDR S-map, we offer a detailed practical guide in SI Text, VII. *Practical guide for applying MDR S-map in empirical analysis*, that helps to improve the quality of network reconstruction in real-world systems. This practical guide addressed three critical issues in analysing empirical dataset, including (i) the selection of informative time series, (ii) the exclusion of rare species from MDR S-map analysis, and (iii) the issue of time series length.

## Concluding remarks

The MDR S-map approach proposed in this study overcame the curse of dimensionality in network reconstruction. This method needs no model assumption and can be used to quantify high-dimensional interaction Jacobian networks using time series data alone. Despite some limitations, the method established on Takens theorem (Takens, 1981) facilitates analysis of datasets exhibiting complex chaotic dynamics generated by nonlinear dynamical systems. This analytical framework can be applied in natural bacteria communities (Figure 3) and easily extended to other real-world systems for searching important nodes or interactions from large networks, if time series of network nodes are available. Therefore, we appeal to collect high-quality time series data from various systems. As such, reconstruction of diverse types of interaction networks is expected to improve our understanding regarding complex interactions and emergent properties of large dynamical networks involving enormous numbers of interacting components.

## ACKNOWLEDGEMENTS

We are grateful for comments from Cheng-Han Tsai and Kazuhiro Takemoto and English editing from John Kastelic that improved our work. This study was supported by National Taiwan University, National Center for Theoretical Sciences, Foundation for the Advancement of Outstanding Scholarship, and Ministry of Science and Technology, Taiwan (to CHH).

## CONFLICT OF INTEREST

The authors declare no competing interests.

## AUTHOR CONTRIBUTIONS

CWC, CHH and TM conceived the research idea; CWC developed the method and analysed the data with

assistance from CHH, MU, PJK and TM; TM constructed the model data; HPL and FKS collected the empirical data; CWC and CHH wrote the manuscript, with critical comments from coauthors.

## PEER REVIEW

The peer review history for this article is available at <https://publons.com/publon/10.1111/ele.13897>.

## OPEN RESEARCH BADGES



This article has earned Open Data, Open Materials and Preregistered badges. Data and materials are available at: <https://www.nature.com/articles/s41467-017-02571-4#Sec24>; [https://github.com/biozoo/MDR\\_S-map](https://github.com/biozoo/MDR_S-map)

## DATA AVAILABILITY STATEMENT

We confirm that this manuscript is not under consideration by another journal and has not been published elsewhere. The empirical bacterial community dataset is open-access. The model used for generating synthetic data and documentations of analytical algorithms is provided as R codes in the Figshare Repository, <https://doi.org/10.6084/m9.figshare.16573037.v1>.

## ORCID

Chun-Wei Chang <https://orcid.org/0000-0002-9817-2956>  
 Takeshi Miki <https://orcid.org/0000-0002-2452-8681>  
 Masayuki Ushio <https://orcid.org/0000-0003-4831-7181>  
 Po-Ju Ke <https://orcid.org/0000-0002-8371-7984>  
 Hsiao-Pei Lu <https://orcid.org/0000-0001-7427-6163>  
 Chih-hao Hsieh <https://orcid.org/0000-0001-5935-7272>

## REFERENCES

- Albert, R., Jeong, H. & Barabási, A.-L. (2000) Error and attack tolerance of complex networks. *Nature*, 406, 378–382.
- Allolina, S. & Levine, J.M. (2011) A competitive network theory of species diversity. *Proceedings of the National Academy of Sciences of the United States of America*, 108, 5638–5642.
- Barbier, M., Arnoldi, J.-F., Bunin, G. & Loreau, M. (2018) Generic assembly patterns in complex ecological communities. *Proceedings of the National Academy of Sciences of the United States of America*, 115, 2156–2161.
- Barrat, A., Barthélemy, M., Pastor-Satorras, R. & Vespignani, A. (2004) The architecture of complex weighted networks. *Proceedings of the National Academy of Sciences of the United States of America*, 101, 3747–3752.
- Bellman, R.E. (1957) *Dynamic programming*. NJ: Princeton University Press.
- Berlow, E.L., Neutel, A.-M., Cohen, J.E., de Ruiter, P.C., Ebenman, B.O., Emmerson, M. et al. (2004) Interaction strengths in food webs: issues and opportunities. *Journal of Animal Ecology*, 73, 585–598.
- Berry, D. & Widder, S. (2014) Deciphering microbial interactions and detecting keystone species with co-occurrence networks. *Frontiers in Microbiology*, 5, 219.
- Bucci, V., Tzen, B., Li, N., Simmons, M., Tanoue, T., Bogart, E. et al. (2016) MDSINE: Microbial Dynamical Systems INference Engine for microbiome time-series analyses. *Genome Biology*, 17, 121.
- Carpenter, S.R. & Kitchell, J.F. (1988) Consumer control of lake productivity. *BioScience*, 38, 764–769.
- Carr, A., Diener, C., Baliga, N.S. & Gibbons, S.M. (2019) Use and abuse of correlation analyses in microbial ecology. *The ISME Journal*, 13, 2647–2655.
- Cenci, S. & Saavedra, S. (2019) Non-parametric estimation of the structural stability of non-equilibrium community dynamics. *Nature Ecology & Evolution*, 3, 912–918.
- Cenci, S., Sugihara, G. & Saavedra, S. (2019) Regularized S-map for inference and forecasting with noisy ecological time series. *Methods in Ecology and Evolution*, 10, 650–660.
- Chang, C.W., Miki, T., Ushio, M., Ke, P.-J., Lu, H.-P., Shiah, F.-K. et al. (2021) Reconstructing large interaction networks from empirical time series data. *Figshare Repository*, Available from: <https://doi.org/10.6084/m9.figshare.16573037.v1>
- Chang, C.-W., Ushio, M. & Hsieh, C.-H. (2017) Empirical dynamic modeling for beginners. *Ecological Research*, 32, 785–796.
- Chang, C.-W., Ye, H., Miki, T., Deyle, E.R., Souissi, S., Anneville, O. et al. (2020) Long-term warming destabilizes aquatic ecosystems through weakening biodiversity-mediated causal networks. *Global Change Biology*, 26, 6413–6423.
- Coheret de la Morinière, E., Pollux, B., Nagelkerken, I., Hemminga, M.A., Huiskes, A. & van der Velde, G. (2003) Ontogenetic dietary changes of coral reef fishes in the mangrove-seagrass-reef continuum: stable isotopes and gut-content analysis. *Marine Ecology Progress Series*, 246, 279–289.
- Craft, C. (2007) Freshwater input structures soil properties, vertical accretion, and nutrient accumulation of Georgia and U.S. tidal marshes. *Limnology and Oceanography*, 52, 1220–1230.
- Csardi, G. & Nepusz, T. (2006) The igraph software package for complex network research. *InterJournal, Complex Systems*, 1695, 1–9.
- Deyle, E.R., Fogarty, M., Hsieh, C.-H., Kaufman, L., MacCall, A.D., Munch, S.B. et al. (2013) Predicting climate effects on Pacific sardine. *Proceedings of the National Academy of Sciences of the United States of America*, 110, 6430–6435.
- Deyle, E.R., May, R.M., Munch, S.B. & Sugihara, G. (2016) Tracking and forecasting ecosystem interactions in real time. *Proceedings of the Royal Society B: Biological Sciences*, 283, 20152258.
- Dunne, J.A., Williams, R.J. & Martinez, N.D. (2002) Food-web structure and network theory: the role of connectance and size. *Proceedings of the National Academy of Sciences of the United States of America*, 99, 12917–12922.
- Fisher, C.K. & Mehta, P. (2014) Identifying keystone species in the human gut microbiome from metagenomic timeseries using sparse linear regression. *PLoS One*, 9, e102451.
- Freilich, M.A., Wieters, E., Broitman, B.R., Marquet, P.A. & Navarrete, S.A. (2018) Species co-occurrence networks: can they reveal trophic and non-trophic interactions in ecological communities? *Ecology*, 99, 690–699.
- Fry, B. (2006) *Stable isotope ecology*. NY: Springer.
- Fuhrman, J.A., Cram, J.A. & Needham, D.M. (2015) Marine microbial community dynamics and their ecological interpretation. *Nature Reviews Microbiology*, 13, 133–146.
- Gonzalez, J.M., Fernandez-Gomez, B., Fernandez-Guerra, A., Gomez-Consarnau, L., Sanchez, O., Coll-Llado, M. et al. (2008) Genome analysis of the proteorhodopsin-containing marine bacterium *Polaribacter* sp. MED152 (Flavobacteria). *Proceedings of the National Academy of Sciences of the United States of America*, 105, 8724–8729.
- Griffin, A.S., West, S.A. & Buckling, A. (2004) Cooperation and competition in pathogenic bacteria. *Nature*, 430, 1024–1027.
- Hastie, T., Tibshirani, R. & Friedman, J. (2009) *The elements of statistical learning: data mining, inference, and prediction*. Springer Science & Business Media.
- Hoegh-Guldberg, O. & Bruno, J.F. (2010) The impact of climate change on the world's marine ecosystems. *Science*, 328, 1523–1528.
- Hsieh, C.-H., Glaser, S.M., Lucas, A.J. & Sugihara, G. (2005) Distinguishing random environmental fluctuations from ecological catastrophes for the North Pacific Ocean. *Nature*, 435, 336–340.

- Kéfi, S., Domínguez-García, V., Donohue, I., Fontaine, C., Thébaud, E. & Dakos, V. (2019) Advancing our understanding of ecological stability. *Ecology Letters*, 22, 1349–1356.
- Kennel, M.B., Brown, R. & Abarbanel, H.D.I. (1992) Determining embedding dimension for phase-space reconstruction using a geometrical construction. *Physical Review A*, 45, 3403–3411.
- Levine, J.M., Bascompte, J., Adler, P.B. & Allesina, S. (2017) Beyond pairwise mechanisms of species coexistence in complex communities. *Nature*, 546, 56.
- Liautaud, K., van Nes, E.H., Barbier, M., Scheffer, M. & Loreau, M. (2019) Superorganisms or loose collections of species? A unifying theory of community patterns along environmental gradients. *Ecology Letters*, 22, 1243–1252.
- Martin-Platero, A.M., Cleary, B., Kauffman, K., Preheim, S.P., McGillicuddy, D.J., Alm, E.J. et al. (2018) High resolution time series reveals cohesive but short-lived communities in coastal plankton. *Nature Communications*, 9, 266.
- McCann, K., Hastings, A. & Huxel, G.R. (1998) Weak trophic interactions and the balance of nature. *Nature*, 395, 794.
- McCoy, S.J. & Pfister, C.A. (2014) Historical comparisons reveal altered competitive interactions in a guild of crustose coralline algae. *Ecology Letters*, 17, 475–483.
- Shalizi, C.R. (2006) Methods and techniques of complex systems science: an overview. In: Deisboeck, T.S. & Kresh, J.Y. (Eds.) *Complex systems science in biomedicine*. US Boston, MA: Springer, pp. 33–114.
- Skelly, D.K. (2002) Experimental venue and estimation of interaction strength. *Ecology*, 83, 2097–2101.
- Song, C. & Saavedra, S. (2021) Bridging parametric and nonparametric measures of species interactions unveils new insights of non-equilibrium dynamics. *Oikos*, 130, 1027–1034.
- Stein, R.R., Bucci, V., Toussaint, N.C., Buffie, C.G., Räscher, G., Pamer, E.G. et al. (2013) Ecological modeling from time-series inference: insight into dynamics and stability of intestinal microbiota. *PLoS Comp. Biol.*, 9, e1003388.
- Strogatz, S.H. (2001) Exploring complex networks. *Nature*, 410, 268–276.
- Sugihara, G., Grenfell, B., May, R.M., Chesson, P., Platt, H.M. & Williamson, M. (1990) Distinguishing error from chaos in ecological time series. *Philosophical Transactions of the Royal Society B*, 330, 235–251.
- Sugihara, G. & May, R.M. (1990) Nonlinear forecasting as a way of distinguishing chaos from measurement error in time series. *Nature*, 344, 734–741.
- Sugihara, G., May, R., Ye, H., Hsieh, C.-H., Deyle, E., Fogarty, M. et al. (2012) Detecting causality in complex ecosystems. *Science*, 338, 496–500.
- Takens, F. (1981). Detecting strange attractors in turbulence. In: Rand, D.A. & Young, L.S. (Eds.) *Dynamical systems and turbulence*. Berlin: Springer, pp. 366–381.
- Ushio, M. (2020). Interaction capacity underpins community diversity. *bioRxiv*, 2020.2004.2008.032524.
- Ushio, M., Hsieh, C.-H., Masuda, R., Deyle, E.R., Ye, H., Chang, C.-W. et al. (2018) Fluctuating interaction network and time-varying stability of a natural fish community. *Nature*, 554, 360–363.
- Ye, H., Clark, A., Deyle, E., Munch, S., Keyes, O. & Cai, J. et al. (2020). rEDM: Applications of empirical dynamic modeling from time series. R package version 1.2.3.
- Ye, H., Deyle, E.R., Gilarranz, L.J. & Sugihara, G. (2015) Distinguishing time-delayed causal interactions using convergent cross mapping. *Scientific Reports*, 5, 14750.
- Ye, H. & Sugihara, G. (2016) Information leverage in interconnected ecosystems: overcoming the curse of dimensionality. *Science*, 353, 922–925.
- Yu, Z., Gan, Z., Huang, H., Zhu, Y. & Meng, F. (2020) The varying bacterial interactions revealed by regularized S-map. *Applied and Environmental Microbiology*, Available from: <https://doi.org/10.1128/AEM.01615-20>
- Zou, H. & Zhang, H.H. (2009) On the adaptive elastic-net with a diverging number of parameters. *The Annals of Statistics*, 37, 1733–1751.

## SUPPORTING INFORMATION

Additional supporting information may be found in the online version of the article at the publisher's website.

**How to cite this article:** Chang, C.-W., Miki, T., Ushio, M., Ke, P.-J., Lu, H.-P., Shiah, F.-K. & et al. (2021) Reconstructing large interaction networks from empirical time series data. *Ecology Letters*, 24, 2763–2774. <https://doi.org/10.1111/ele.13897>